Mathematical Biosciences 310 (2019) 65–75

Contents lists available at ScienceDirect

Mathematical Biosciences

journal homepage: www.elsevier.com/locate/mbs

Structured mathematical models to investigate the interactions between *Plasmodium falciparum* malaria parasites and host immune response

Baoling Ma[*,a], Chuan Li[b], Jack Warner[a]

[a] Department of Mathematics, Millersville University of Pennsylvania, Millersville, PA 17551, USA
[b] Department of Mathematics, West Chester University of Pennsylvania, West Chester, PA 19382, USA

ARTICLE INFO

Keywords:
Structured population models
Erythropoiesis
Malaria
Plasmodium falciparum
Immune cells
Antibodies
Finite difference scheme
Severe infection
Drug treatment

ABSTRACT

Malaria infection has posed a major health threat for hundreds of years in human history. Yet, due to the complex interactions between a host immune response and the parasite, no sophisticated mathematical models exist to study its dynamics. In this work, we propose a new system of structured partial differential equations that account for the dependence of red blood cell infectivity on maturation level. These equations are coupled with another set of differential equations for investigating the population dynamics of *Plasmodium falciparum* and its interaction with red blood cells and cells of the immune system. A finite difference scheme is developed to solve the system. Numerical simulations are applied to investigate the interplay between the host immune response and the parasite dynamics, the disease dynamics in acute infection, and treatment effectiveness with different drugs.

1. Introduction

In 2013, the World Malaria Report estimated that 207 million clinical episodes, and 627,000 deaths were caused by malaria in 2012 [40], indicating malaria has been a constant threat to more than 40% of children all over the world. Young children are most vulnerable to this disease and many deaths are due to the lack of effective treatments [13,17,28]. Malaria is caused by parasites which are transmitted through the bite of an infected Anopheles mosquito. Of the four human malarial species, *Plasmodium falciparum* is by far the deadliest [31,32].

Due to its status as a major health threat to human beings, there has been a rise in research of this deadly infection in recent decades. The mathematics community has joined the effort and has applied several approaches towards understanding the disease. A large percentage of these applications have been focused on the dynamics of the malaria parasite within an infected host using mathematical models [2,3,9,14–16,18,19,25,34,36,37]. For instance, an age-structured mathematical model is developed in [36] to study the population dynamics of malaria parasites and their interactions with immune cells. The developed model consists of a system of delay differential equations to incorporate a time delay between the infection of red blood cells (RBCs) by the merozoites and the release of merozoites for the next generation. A mathematical model is proposed in [29] for simulating severe malaria infections based on the hypothesis that malaria parasites can be absorbed in already infected RBCs due to the restrained availability of uninfected RBCs to merozoites. This model consists of four ordinary differential equations that describe the dynamics of RBCs, first time infected RBCs, double infected RBCs, and merozoites. Meanwhile, a Markov chain Monte Carlo method is adopted in this model to study parameter identifiability and model behavior. In [7] an intra-host model of immune response to *Plasmodium falciparum* infection is proposed and then this model is extended to include treatment with anti-malarial drugs. In [21] a system of differential equations is developed to analyze the dynamics of blood stage malaria with immune response and the effectiveness of drugs in the treatment of *Plasmodium falciparum* malaria infection. In all of the above mentioned models the release of RBCs is assumed to be at a constant rate.

In this work, a novel model is developed to study the population dynamics of *Plasmodium falciparum* and its interaction with the process of RBC production and the immune system. The mathematical model is formulated as structured partial differential equations to account for the dependence of RBC infectivity on its maturation level. The model is then extended to investigate the disease dynamics in the case of severe infection by incorporating the hypothesis that merozoites get absorbed into already infected RBCs when there is a limited supply of uninfected RBCs in the acute infection. A high-resolution finite difference scheme is developed to solve the model numerically. Biological simulations are performed to investigate the disease dynamics of the within-host

* Corresponding author.
E-mail addresses: baoling.ma@millersville.edu (B. Ma), cli@wcupa.edu (C. Li), jmwarne3@millersville.edu (J. Warner).

https://doi.org/10.1016/j.mbs.2019.02.005
Received 8 January 2018; Received in revised form 10 August 2018; Accepted 12 February 2019
Available online 13 February 2019

malaria infection, the impact of the infection on the RBC production process, and the response of the immune system to the infection. The behaviors of the complex within-host system in the case of severe infection and under antimalarial drug treatment are also studied. The models and the numerical methods provide a useful tool to investigate the impact of a variety of disease parameters within the parasite dynamics, as well as insights to efficient control strategies of the disease in various scenarios. For instance, one can conduct simulations to identify crucial experimental parameters for studying the interplay between the host immune response and the parasite. To our best knowledge, this is the first study that incorporates the interplay and the erythropoiesis process together to investigate a severe infection scenario within the complex within-host system and under anti-malaria drug treatment.

The rest of this work is organized as follows. In Section 2, a new mathematical model for studying host-parasite interactions is provided and numerically investigated. In Section 3, the model is extended to gain some understanding of severe malaria by imposing a mathematical hypothesis. Conclusion and discussion of this work are provided in Section 4.

2. A new structured mathematical model for studying host-parasite interactions

2.1. The mathematical model

Natural transmission of malaria occurs when a human host is exposed to the bite of an infective female anopheline mosquito. Recent studies using intravital imaging have shown that sporozoites are injected by mosquitoes into the skin, where they can remain for up to 6 hours, and that approximately one-third of those leaving the skin may enter lymphatics and drain to the regional lymph nodes; other sporozoites trickle into the bloodstream and traffic to the liver, resulting in multiple potential sites for sporozoite-host interaction ([10] and Refs. therein). The interaction among RBCs, malaria parasites, and the host immune system in this process is shown in Fig. 1. Further details will follow.

Seven population and population density variables are taken into consideration in the proposed models. Their interpretations are listed in Table 1. For each of these seven variables, a differential equation is established accounting for a specific biological process to describe its changes with respect to individual independent variables.

We establish the model starting with the RBC production process. When detecting low oxygen levels in the blood stream, the host's body responds by releasing erythropoietin, a hormone produced primarily by the kidney, at a rate of f which is assumed to depend on the RBC population, M. Erythropoietin decays at a rate denoted by α_E. The erythropoietin concentration, $E(t)$, is therefore modeled by the differential equation

$$\frac{dE(t)}{dt} = f(t, M(t)) - \alpha_E(t, P(t))E(t), \tag{2.1}$$

Table 1
Model variables.

Variable	Interpretation
$p(t, \mu)$	Density of precursor cells at time t with maturation level μ
$m(t, \nu)$	Density of healthy mature red blood cells (RBC) of age ν at time t
$E(t)$	Erythropoietin concentration at time t
$X(t)$	Number of infected red blood cells at time t
$Y(t)$	Concentration of merozoite at time t
$I(t)$	Concentration of immune cells at time t
$A(t)$	Concentration of antibodies at time t

where $P(t) = \int_0^{\mu_F} p(t, \mu)d\mu$ is the precursor population.

The hormone erythropoietin triggers the stem cells in the bone marrow to join the RBC precursor population. The recruitment of stem cells is assumed to be proportional to the erythropoietin concentration in our model and is described by the boundary condition

$$g(E(t))p(t, 0) = \phi(t)E(t), \tag{2.2}$$

where $\phi(t)$ is the proportionality coefficient function and g is the precursor growth rate.

Malaria parasites do not infect precursors. However, it was found that infected RBCs release a toxin that suppresses precursor production [6]. To this end, we model the dynamics of precursor density by a partial differential equation

$$\frac{\partial p(t, \mu)}{\partial t} + g(E(t))\frac{\partial p(t, \mu)}{\partial \mu} = \sigma(t, \mu, E(t))p(t, \mu) - H(X(t))p(t, \mu), \tag{2.3}$$

where σ is the net results of precursor birth (mitosis during the beginning of maturation phase) and natural mortality rate, and H is a rate of reduction.

Once the precursor reaches the maximum maturation level, μ_F, it leaves the bone marrow and joins the RBC population. It is assumed that the supply rate of RBCs is accelerated by the presence of infected RBCs, although the mechanisms regarding the acceleration are still poorly understood [41]. We simply model this acceleration rate by the term $k_0X(t)$ with $0 \le k_0 < 1$. The age-dependent natural mortality rate of RBC is denoted by α_m. We assume this mortality rate also depends on the population of mature RBCs, M. Free merozoites in the blood stream seek to infect RBCs at a rate modeled by k_s. Antibodies specific to malaria parasites inhibit the invasion of erythrocytes by merozoites. Thus the infection rate, k_s, depends on $A(t)$. In this work the infection rate is modeled as $k_s(t, A(t)) = \frac{k_1}{1 + k_2A(t)}$, where k_1 is the rate of infection in the absence of antibody inhibition, and k_2 describes the efficiency of antibodies at reducing erythrocytic invasion. RBCs are recruited through the maturation of precursors modeled by

$$m(t, 0) = g(E(t))p(t, \mu_F). \tag{2.4}$$

Provided above assumptions, the dynamics of RBC density is thereby modeled by the partial differential equation

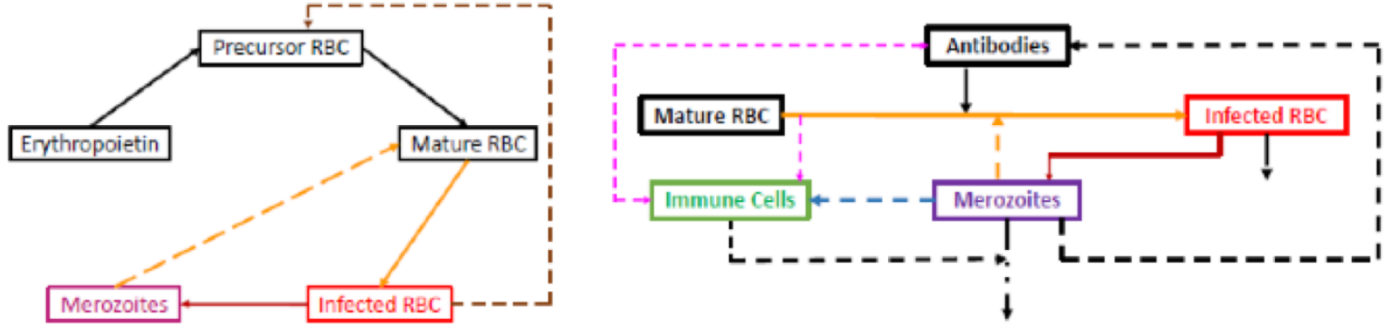

Fig. 1. Model diagram for the interaction among erythropoietin, precursor, mature RBC, merozoites, infected RBC, immune cells, and antibodies.

$$\frac{\partial m(t,\nu)}{\partial t}+\frac{\partial m(t,\nu)}{\partial \nu}=k_0X(t)-\alpha_m(t,\nu,M(t))m(t,\nu)-\frac{k_1}{1+k_2A(t)}Y(t)m(t,\nu), \tag{2.5}$$

where $M(t)=\int_0^{\nu_F} m(t,\nu)d\nu$ is the total population of RBCs.

Once a free merozoite enters the host blood stream, it seeks to infect a healthy RBC. Infected RBCs travel throughout the blood stream while parasites duplicate within them. After a certain time, the cell bursts (at a rate of $s(t)$) and releases a number of new parasites into the blood stream which seek to continue the process. Infected RBCs experience a constant mortality rate which is denoted by α_x. Infected RBCs are also killed by immune cells with a rate modeled by $k_3I(t)X(t)$ due to the immunosensitivity of infected RBCs [26]. In the light of the above process, the dynamics of infected RBCs is modeled by

$$\frac{dX(t)}{dt}=\frac{k_1}{1+k_2A(t)}Y(t)M(t)-s(t)X(t)-\alpha_xX(t)-k_3I(t)X(t). \tag{2.6}$$

A number of new merozoites are released into the blood stream when an infected RBC bursts. We denote by r the average number of merozoites released per bursting infected RBC when no immune exists. Immune cells suppress this parasite production with efficiency k_4. Merozoites suffer from a natural mortality rate, α_y, and some are killed by immune cells with efficiency k_5. The merozoite population is also reduced through the infection of RBCs. Combining the above interactions we model the dynamics of merozoites by

$$\frac{dY(t)}{dt}=\frac{r}{1+k_4I(t)}s(t)X(t)-\alpha_yY(t)-k_5I(t)Y(t)-\frac{k_1}{1+k_2A(t)}Y(t)M(t). \tag{2.7}$$

The human immune system reacts to the presence of malaria parasites and releases many different types of immune cells. Recruitment of immune cells is stimulated by the presence of infected RBCs and merozoites. For the sake of simplicity, we treat all immune cells as one population and model the change of immune population by

$$\frac{dI(t)}{dt}=\lambda_I(t)+\left(\frac{\lambda_xX(t)}{k_6+X(t)}+\frac{\lambda_yY(t)}{k_7+Y(t)}\right)I(t)-\alpha_II(t), \tag{2.8}$$

where $\lambda_I(t)$ is the host's rate of producing immune cells, λ_x and λ_y denote the immunogenicity of infected RBC and merozoites, respectively, and α_I is the mortality rate of immune cells. We denote by k_6 the population of infected RBC at which the immune cells grow at $\lambda_x/2$ in the absence of merozoites, and by k_7 the population of merozoites at which the immune cells grow at $\lambda_y/2$ in the absence of infected RBC.

Finally, antibodies that block the invasion of RBCs by merozoites are secreted mainly by immune cells when merozoites are present [4]. We denoted by η the maximum reproduction rate of antibodies. Antibodies are proteins that travel around in the bloodstream, recognize parasites, and bind to them [20]. The decay rate of antibodies in the blood stream thus depends on the parasite population. We model their decay rate by $\alpha_AA(t)Y(t)$. We introduce the last differential equation for describing the change of antibody population as

$$\frac{dA(t)}{dt}=\eta I(t)\frac{Y(t)}{k_8+Y(t)}-\alpha_AA(t)Y(t). \tag{2.9}$$

Here, k_8 denotes the population of merozoites at which the antibodies grow at 50% of its maximum growth rate η.

Grouping the above mentioned equations together yields the first model (**model I**):

$$\begin{aligned}
\frac{dE(t)}{dt} &= f(t,M(t))-\alpha_E(t,P(t))E(t),\\
\frac{\partial p(t,\mu)}{\partial t}+g(E(t))\frac{\partial p(t,\mu)}{\partial \mu} &= \sigma(t,\mu,E(t))p(t,\mu)-H(X(t))p(t,\mu),\\
& \quad 0<\mu<\mu_F,\\
\frac{\partial m(t,\nu)}{\partial t}+\frac{\partial m(t,\nu)}{\partial \nu} &= k_0X(t)-\alpha_m(t,\nu,M(t))m(t,\nu)\\
& \quad -\frac{k_1}{1+k_2A(t)}Y(t)m(t,\nu),\\
& \quad 0<\nu<\nu_F,\\
\frac{dX(t)}{dt} &= \frac{k_1}{1+k_2A(t)}Y(t)M(t)-s(t)X(t)\\
& \quad -\alpha_xX(t)-k_3I(t)X(t),\\
\frac{dY(t)}{dt} &= \frac{r}{1+k_4I(t)}s(t)X(t)-\alpha_yY(t)\\
& \quad -k_5I(t)Y(t)\\
& \quad -\frac{k_1}{1+k_2A(t)}Y(t)M(t),\\
\frac{dI(t)}{dt} &= \lambda_I(t)+\left(\frac{\lambda_xX(t)}{k_6+X(t)}+\frac{\lambda_yY(t)}{k_7+Y(t)}\right)I(t)\\
& \quad -\alpha_II(t),\\
\frac{dA(t)}{dt} &= \eta I(t)\frac{Y(t)}{k_8+Y(t)}-\alpha_AA(t)Y(t),
\end{aligned} \tag{2.10}$$

with the following imposed boundary and initial conditions

$$\begin{aligned}
g(E(t))p(t,0) &= \phi(t)E(t),\\
m(t,0) &= g(E(t))p(t,\mu_F),\\
p(0,\mu) &= p^0(\mu),\quad 0\le\mu\le\mu_F,\\
m(0,\nu) &= m^0(\nu),\quad 0\le\nu\le\nu_F,\\
E(0) &= E^0,\ X(0)=X^0,\ Y(0)=Y^0,\ I(0)=I^0,\\
A(0) &= A^0
\end{aligned} \tag{2.11}$$

For easy reference, detailed descriptions of involved parameters and their biological meanings are provided in Table 2.

2.2. A finite difference algorithm

The exact solution to Model I is analytically intractable due to its complexity. We therefore seek numerical approximations to investigate the quantitative properties of the model and study interactions between host erythropoiesis, immune responses, and malaria parasites. In the numerical process, it is important to keep in mind that the outputs of the model are population size and densities, so that the numerical solutions must be nonnegative. Moreover, the numerical approaches are expected to be efficient, deliver accurate approximations to the exact solutions, and be capable of resolving possible noncompatible initial and boundary conditions arising from experimentally obtained raw data.

The following notations are used for describing the proposed numerical method. Let the whole simulation time interval $[0, T]$ be discretized by an uniform temporal increment Δt into L equally-spaced time subintervals, i.e., $\Delta t=T/L$, such that $t_k=k\Delta t$ for $k=0,\ldots,L$. Similar discretization is applied to discretize intervals $[0,\mu_F]$ and $[0,\nu_F]$ with uniform mesh sizes $\Delta\mu$, $\Delta\nu$, yielding n_1 and n_2 equally spaced subintervals, respectively, such that $\mu_i=i\Delta\mu$ for $i=0,\ldots,n_1$, and $\nu_j=j\Delta\nu$ for $j=0,\ldots,n_2$. We denote the numerical approximations to the exact values of $E(t_k)$, $p(t_k,\mu_i)$, $m(t_k,\nu_j)$, $P(t_k)$, $m(t_k)$, $X(t_k)$, $Y(t_k)$, $I(t_k)$, and $A(t_k)$, by E^k, p_i^k, m_j^k, P^k, M^k, X^k, Y^k, I^k, and A^k, respectively.

Table 2
Description of model parameters.

$f(t, M(t))$	Releasing rate of erythropoietin from the kidney
$\alpha_E(t, P(t))$	The decay rate of erythropoietin
$g(E(t))$	Precursor growth rate
$\phi(t)$	The proportionality coefficient function.
$\sigma(t, \nu, E(t))$	Net results of birth (mitosis during the beginning of maturation phase) and natural mortality rate
$H(X(t))$	The rate at which infected RBC suppresses precursor production.
k_0	Rate of recruitment of RBCs due to the presence of infected RBCs.
$\alpha_m(t, \nu, M(t))$	The mortality rate of mature RBCs.
k_1	Parasite infection rate in the absence of antibodies
k_2	Efficiency of antibodies
$s(t)$	The bursting rate of infected RBC
α_x	The mortality rate of infected RBC
k_3	Immunosensitivity of infected RBCs
r	The average number of merozoite released after one burst
k_4	Efficiency of immune cells at supressing the parasite production
α_y	Removal rate of free merozoite through mortality
k_5	Immunosensitivity of merozoites
$\lambda_I(t)$	Rate at which immune cells are produced by the host
λ_x	The immunogenicity of infected RBC
λ_y	The immunogenicity of merozoites
α_I	The mortality rate of immune cells
k_6	Infected RBC population at which the immune cells grow at $\lambda_x/2$ in the absence of merozoites
k_7	Merozoites population at which the immune cells grow at $\lambda_y/2$ in the absence of infected RBC
η	Maximum reproduction rate of antibodies
α_A	Decay rate of antibodies
k_8	Merozoites population at which the antibodies grow at 50% of its maximum growth rate η

Finally, we denote $f^k = f(t^k)$, $\alpha_E^k = \alpha_E(t^k)$, $g^k = g(E(t^k))$, $\sigma_i^k = \sigma(t^k, \nu_i, E(t^k))$, $H^k = H(X(t^k))$, and other notations follow the same fashion.

Given above notations, we utilize the first order finite difference method to discretize model I (2.10)-(2.11) and obtain

$$\begin{aligned}
\frac{E^{k+1}-E^k}{\Delta t} &= f^k - \alpha_E^k E^{k+1},\\
\frac{p_i^{k+1}-p_i^k}{\Delta t} + g^{k+1}\frac{p_i^k - p_{i-1}^k}{\Delta \mu} &= \sigma_i^{k+1} p_i^k - H^k p_i^{k+1}, \quad i = 1, \ldots, n_1,\\
\frac{m_j^{k+1}-m_j^k}{\Delta t} + \frac{m_j^k - m_{j-1}^k}{\Delta \nu} &= k_0 X^k - (\alpha_m)_j^k m_j^{k+1} - \frac{k_1}{1+k_2 A^k} Y^k m_j^{k+1},\\
& \quad j = 1, \ldots, n_2,\\
\frac{X^{k+1}-X^k}{\Delta t} &= \frac{k_1}{1+k_2 A^k} Y^k M^{k+1} - s^{k+1} X^{k+1} - \alpha_x X^{k+1}\\
& \quad - k_3 I^k X^{k+1},\\
\frac{Y^{k+1}-Y^k}{\Delta t} &= \frac{r}{1+k_4 I^k} s^{k+1} X^{k+1} - \alpha_y Y^{k+1} - k_5 I^k Y^{k+1}\\
& \quad - \frac{k_1}{1+k_2 A^k} Y^{k+1} M^{k+1},\\
\frac{I^{k+1}-I^k}{\Delta t} &= \lambda_I{}^{k+1} + \left(\frac{\lambda_x X^{k+1}}{k_6 + X^{k+1}} + \frac{\lambda_y Y^{k+1}}{k_7 + Y^{k+1}}\right) I^k\\
& \quad - \alpha_I I^{k+1},\\
\frac{A^{k+1}-A^k}{\Delta t} &= \eta I^{k+1} \frac{Y^{k+1}}{k_8 + Y^{k+1}} - \alpha_A A^{k+1} Y^{k+1},\\
g^{k+1} p_0^{k+1} &= \phi^{k+1} E^{k+1},\\
m_0^{k+1} &= g^{k+1} p_{n_1}^{k+1}.
\end{aligned} \tag{2.12}$$

Regrouping terms in (2.12) yields

$$\begin{aligned}
E^{k+1} &= (E^k + f^k \Delta t)/(1 + \alpha_E^k \Delta t),\\
p_i^{k+1} &= \left(\left(1 - \frac{\Delta t}{\Delta \mu} g^{k+1} + \sigma_i^{k+1} \Delta t\right) p_i^k + \frac{\Delta t}{\Delta \mu} g^{k+1} p_{i-1}^k\right)/(1 + H^k \Delta t),\\
& \quad i = 1, \ldots, n_1,\\
m_j^{k+1} &= \left(m_j^k \left(1 - \frac{\Delta t}{\Delta \nu}\right) + \frac{\Delta t}{\Delta \nu} m_{j-1}^k + k_0 X^k \Delta t\right)\\
& \quad \Big/\left(1 + (\alpha_m)_j^k \Delta t + \frac{k_1}{1+k_2 A^k} Y^k \Delta t\right),\\
& \quad j = 1, \ldots, n_2,\\
X^{k+1} &= \left(X^k + \frac{k_1}{1+k_2 A^k} Y^k M^{k+1} \Delta t\right)/(1 + s^{k+1} \Delta t + \alpha_x \Delta t + k_3 I^k \Delta t),\\
Y^{k+1} &= \left(Y^k + \frac{r}{1+k_4 I^k} s^{k+1} X^{k+1} \Delta t\right)\Big/\left(1 + \alpha_y \Delta t + k_5 I^k \Delta t\right.\\
& \quad \left. + \frac{k_1}{1+k_2 A^k} M^{k+1} \Delta t\right),\\
I^{k+1} &= \left(I^k + \lambda_I{}^{k+1} \Delta t + \left(\frac{\lambda_x X^{k+1}}{k_6 + X^{k+1}} + \frac{\lambda_y Y^{k+1}}{k_7 + Y^{k+1}}\right) I^k \Delta t\right)/(1 + \alpha_I \Delta t),\\
A^{k+1} &= \left(A^k + \eta I^{k+1} \frac{Y^{k+1}}{k_8 + Y^{k+1}} \Delta t\right)/(1 + \alpha_A Y^{k+1} \Delta t),\\
p_0^{k+1} &= (\phi^{k+1} E^{k+1})/g^{k+1},\\
m_0^{k+1} &= g^{k+1} p_{n_1}^{k+1},
\end{aligned} \tag{2.13}$$

Coupling (2.12) and (2.13) with initial conditions

$$\begin{aligned}
p_i^0 &= p^0(\mu_i), \quad i = 0, \ldots, n_1,\\
m_j^0 &= m^0(\nu_j), \quad j = 0, \ldots, n_2,\\
E(0) &= E^0, X(0) = X^0, Y(0) = Y^0, I(0) = I^0, A(0) = A^0,
\end{aligned} \tag{2.14}$$

delivers the desired finite difference scheme for solving model I.

2.3. Simulation results

We utilize numerical schemes (2.13) and (2.14), together with the parameter values listed in Table 3, to study the interactions among RBCs, malaria parasites, and host immune responses.

In all results described below, the unit for precursor population $P(t)$ is cells per kg body weight $\times 10^{11}$, the unit for mature RBC population is cells per kg body weight $\times 10^{11}$, the units for infected RBC is cells per kg body weight, and the unit for E is mU/mL.

(i) Effect of host immune responses

Shortly following a first time infection, it is assumed that there is no immunity. After surviving the infection, patients develop a certain level of immunity. Firstly, we investigate how the host innate and adaptive immune responses affect the disease dynamics without treatment. Fig. 2 shows that the natural host immune responses can slightly reduce the number of infected RBCs and merozoites, but the defense of the immune system is not able to neutralize the malaria infection. After the infection, the RBC level experiences a sharp drop and stays at a low level afterwards.

(ii) Effect of parasites vital rates

Next, we investigate the impact of various vital rates of the parasites on the disease dynamics. There are various approaches to reduce merozoite infection such as reducing the number of free merozoites released per bursting infected RBC, r, or increasing parasite mortality, α_y. We simulate different changes on the parasite vital rates to investigate the sensitivity of the system to these rates. Fig. 3 shows that the total healthy RBC population is clearly affected by the number of free merozoites released by one infected RBC per burst. It seems that a 25% reduction in r reduces the merozoites population by almost 50%, and a 75% reduction in r will neutralize the disease infection and keep

Table 3
Parameter values and their dimensions.

Parameter	Units	Value	Source
T	days	20	
μ_F	maturity level	5.9	[5,23]
ν_F	days	120	[34]
$f(t, M(t))$	$days^{-1}$	$\frac{15600}{1+0.0382M^{6.96}}$	[34]
$\alpha_E(P)$	$days^{-1}$	$\frac{13.8P+0.04}{0.08+P}$	[1,34]
$g(E)$	maturity level / day	$\frac{3.02E+0.31}{30.61+E}$	[1,34]
$\phi(t)$		4.45×10^{-7}	[34]
$\sigma(t, \mu, E)$	$days^{-1}$	$g(E)\left(\frac{2.773}{1+\exp[4(\mu-3)]} - \frac{0.5}{1+E}\right)$	[1]
$H(X)$	$days^{-1}$	$\frac{0.11X}{X+1}$	[6]
k_0	cells $days^{-1}$	9.0×10^{-5}	estimated
$\alpha_m(t, \nu, M)$	$days^{-1}$	0.0083	[3]
k_1		2.0×10^{-9}	[36]
k_2	μl	6.0×10^{-4}	estimated
$s(t)$	$days^{-1}$	$0.5\sin^2(\pi t/2)$	[30]
α_x	$days^{-1}$	0.025	[37]
k_3	cell $\times$ μl $\times$ d	10^{-8}	estimated
r	parasites/infected RBC	16	[16,37]
k_4	cell $\times$ μl	8.5×10^{-4}	estimated
α_y	$days^{-1}$	48	[37]
k_5	d^{-1}	10^{-8}	[3]
λ_I	$c \times \mu l \times d^{-1}$	10.0	estimated
λ_x	$days^{-1}$	0.05	[7]
λ_y	$days^{-1}$	0.05	[7]
α_I	$days^{-1}$	0.05	[3]
k_6	$\mu l \times c^{-1}$	2000	[7]
k_7	$\mu l \times m^{-1}$	1500	[7]
η	$days^{-1}$	0.6	[7]
α_A	$days^{-1}$	5.0×10^{-10}	[7]
k_8	$\mu l \times m^{-1}$	1500	[7]
$p^0(\mu)$	cells/maturity level $\times 10^{11}$	$\begin{cases}0.0025\mu 0 \le \mu \le 3\\0.0075\mu > 3\end{cases}$	estimated
$m^0(\nu)$	cells/age $\times 10^{11}$	0.025	estimated
E^0	mU/mL	15	[34]
X^0	cells / kg body weighy $\times 10^{11}$	0	estimated
Y^0		2×10^5	estimated
I^0		10^{-2}	estimated
A^0		0	estimated

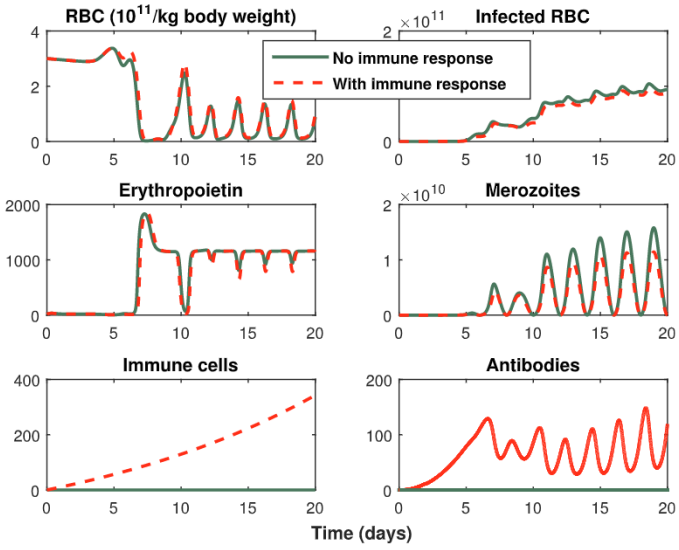

Fig. 2. Comparison of the dynamics with/without host immune responses.

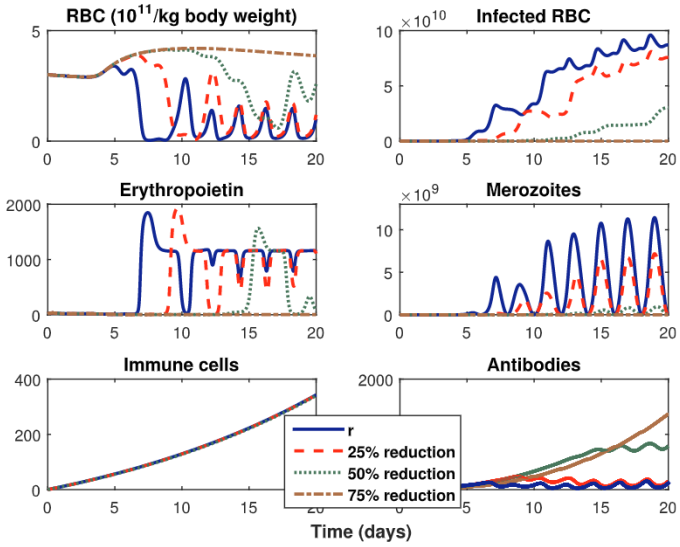

Fig. 3. Effect of reducing the free parasites per bursting infected erythrocyte (r) on the disease dynamics.

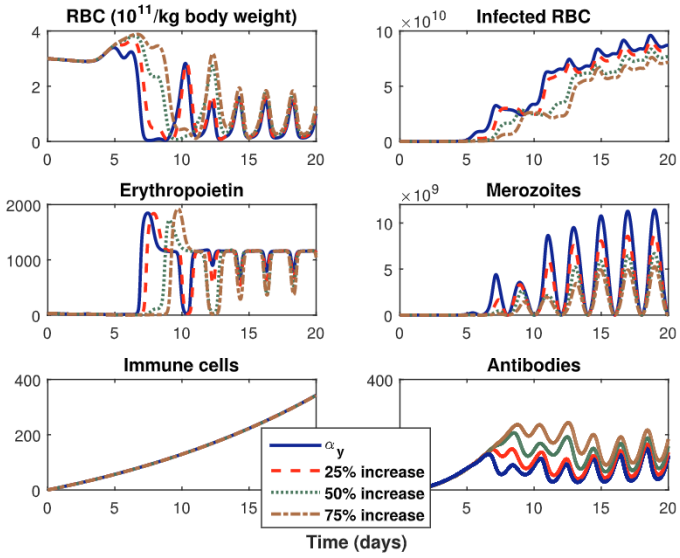

Fig. 4. The effect of increasing parasite mortality rate (α_y) on the disease dynamics.

the RBC population at a healthy level. Figs. 4 and 5 demonstrate that the disease dynamics is also very sensitive to parasite mortality rate α_y and parasite infection rate k_1. However, reducing the number of free merozoites released per infected RBC (r) seems to be the most effective way of maintaining a healthy population of RBCs and controlling the disease. These simulation results are consistent with prior studies in literature [1,2,29]. The rate that describes the impact of parasites on RBC production, k_0, does not affect the disease dynamics noticeably, as shown in Fig. 6.

(iii) Effect of immune cell protection and antibody prevention

We then simulate how host immune cells and antibodies would affect the disease infection if the host innate and adaptive immune responses become more effective. As demonstrated in Figs. 7–10, the numerical results show that simply strengthening the immune system does not put the infection under control. Increasing the immunosensitivity of infected RBC and merozoites (denoted by k_3 and k_5 respectively) does not reduce the infection level, nor does it keep the RBC at a healthy level. When improving the immunogenicity of infected RBC (λ_x) or merozoites (λ_y), the secretion of immune cells gets faster,

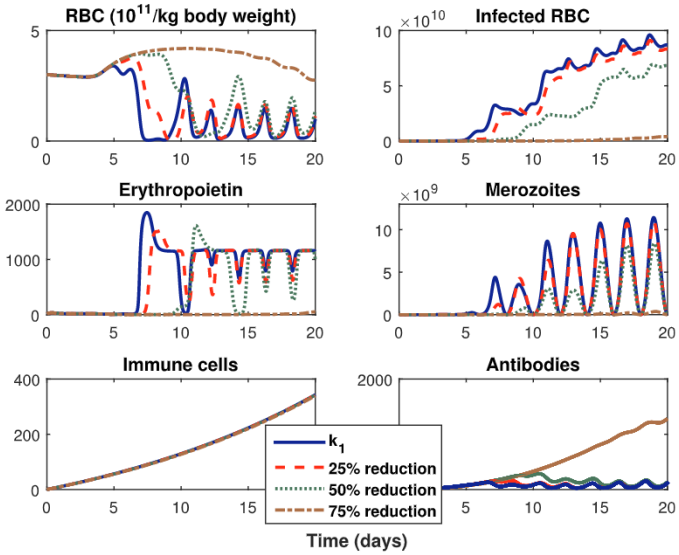

Fig. 5. The effect of reducing the maximum infection rate of the parasites (k_1) on the disease dynamics.

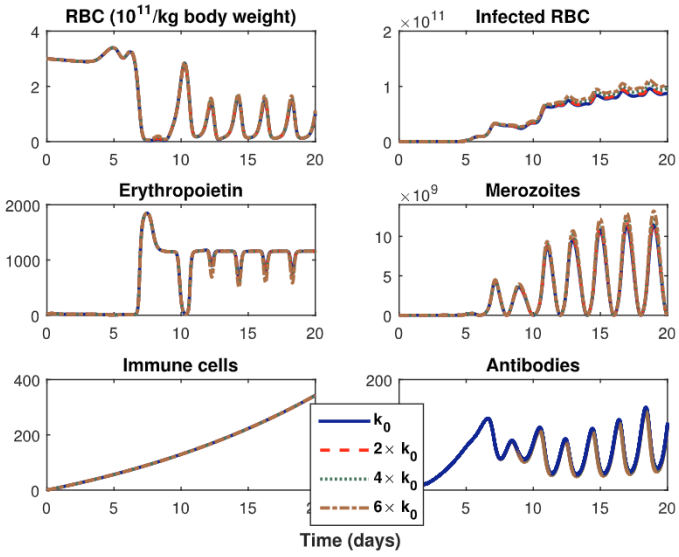

Fig. 6. The effect of malaria infection on erythropoiesis process (k_0) on the disease dynamics.

which results in a slow decrease in the population of infected RBC and merozoites. However, this does not maintain a healthy level of RBC population. When increasing the efficiency of antibodies in blocking the parasite infection of healthy RBCs, k_2, or increasing the reproduction rate of antibodies, η, by 75%, the infected RBC and merozoite population experience only a slight decrease.

2.4. Investigation of efficient treatment strategies

(i) Treatment with Sulfadoxine/Pyrimethamine (SP) or Artemether/lumefantrine

Intermittent preventive treatment in pregnancy (IPTP) with sulfadoxine/pyrimethamine has proven efficacious in reducing the incidence of pregnancy-associated malaria [39]. It is recommended for all pregnant women in most countries in Africa [22,33], although there exist concerns that sulfadoxine/pyrimethamine now demonstrates inadequate therapeutic efficacy due to an increasing resistance to sulfadoxine/pyrimethamine [12]. SP works by blocking the formation of

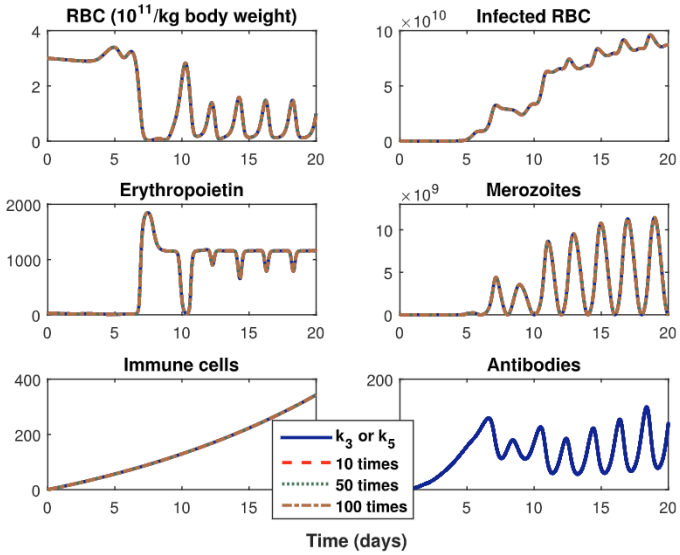

Fig. 7. The effect of immunosensitivity of infected RBC (k_3) and merozoites (k_5) on the disease dynamics.

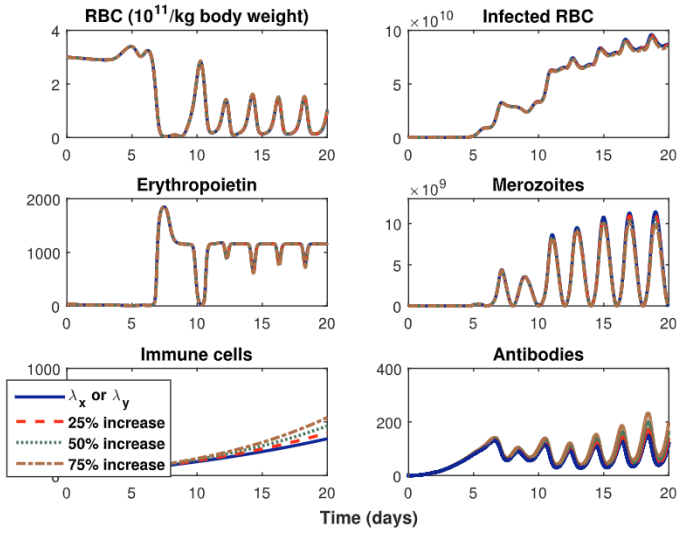

Fig. 8. Impact of immunogenicity of infected RBC (λ_x) and merozoites (λ_y) on the disease dynamics.

folinic acid within the malaria organism, which kills the parasite.

Artemether/lumefantrine, sold under the trade name Coartem, is a prescription medication used to treat acute uncomplicated malaria infections due to *Plasmodium falciparum*. It provides effective treatment for children with uncomplicated *Plasmodium falciparum* infection in areas with highly endemic and multidrug-resistant malaria [11]. Coartem acts against the erythrocytic stage of malaria infection the same way as SP.

When SP or Coartem is administered, the number of merozoites released by one burst infected RBC, r, is reduced to $(1-\gamma)r$, where γ represents the drug efficacy. To incorporate the drug efficacy in the mathematical model, we modify the 5th equation in model I (2.10) as below and keep the other equations the same.

$$\frac{dY(t)}{dt} = \frac{(1-\gamma)r}{1+k_4 I(t)} s(t)X(t) - \alpha_y(t)Y(t) - k_5 I(t)Y(t) - \frac{k_1}{1+k_2 A(t)} Y(t)M(t), \tag{2.15}$$

Fig. 11 shows that the administration of the drug SP or Coartem will

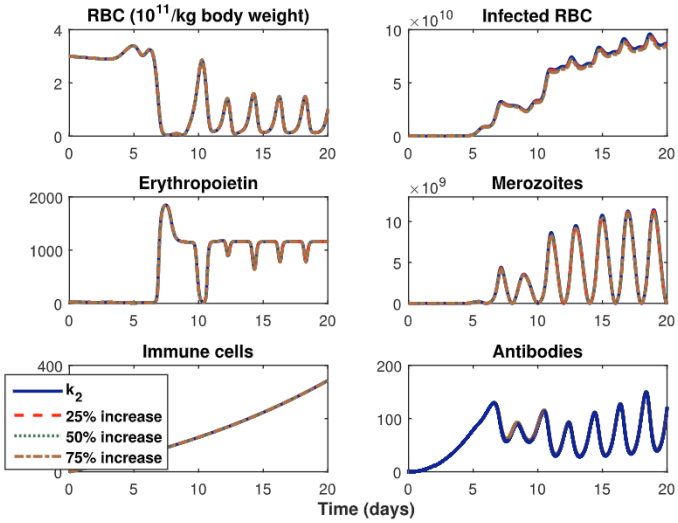

Fig. 9. Impact of efficiency of antibodies in blocking parasites infecting RBC (k_2) on the disease dynamics.

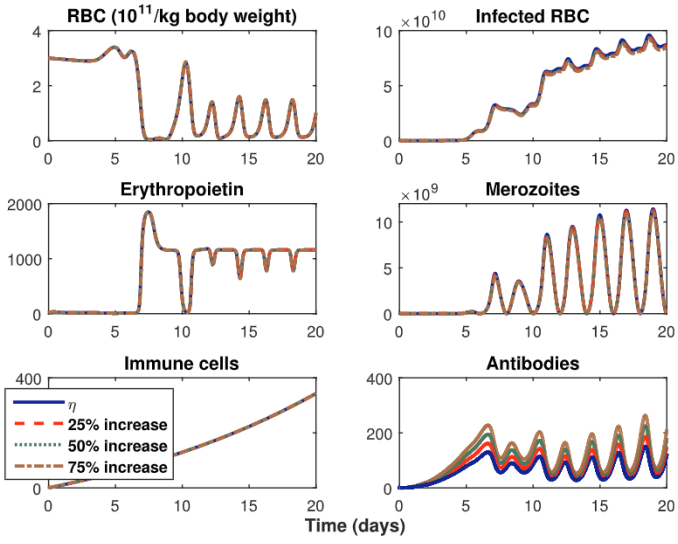

Fig. 10. Impact of the reproduction rate of antibodies (η) on the disease dynamics.

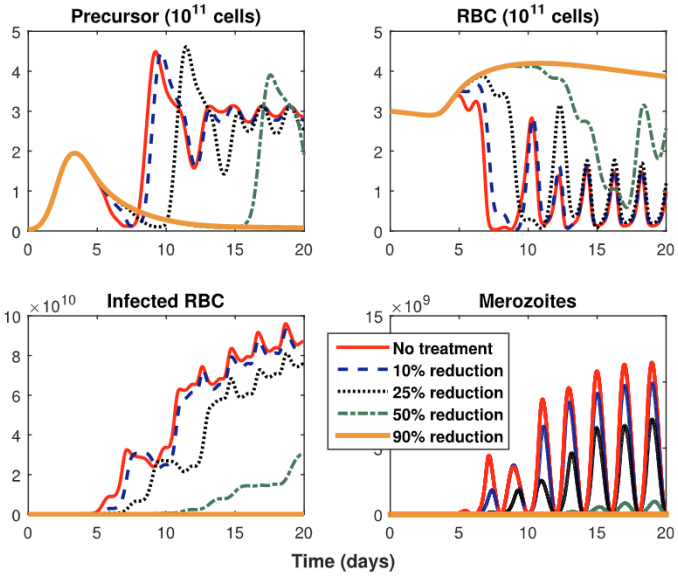

Fig. 11. Treatment effects of SP or Coartem.

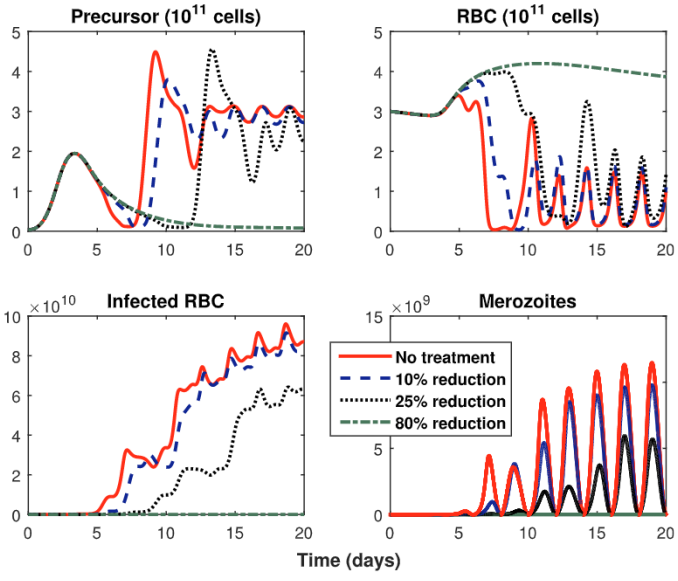

Fig. 12. Treatment effects of Malarone.

effectively control the disease. Specifically, when the drug efficacy reaches 50%, the level of infection is shown to be very low in the first two weeks. After that, however, the population of infected RBCs and merozoites climb up while the RBC level goes down graduallly. When the drug efficacy gets to 90%, parasites are cleared and the RBC level remains at a stable healthy level. Our simulation result is close to the clinical treatment result where the drug efficacy was 0.946 ([27]) for uncomplicated malaria caused by *Plasmodium falciparum*.

(ii) Treatment with Atovaquone–Proguanil

Atovaquone–Proguanil, commercially known as Malarone, is a drug used to treat or prevent malaria. Malarone has been the principal treatment of acute malaria since it was marketed in 2001 [8]. It is active against malaria infection during the blood and exoerythrocytic stage. Treatment with Malarone reduces the infection rate k_1 of RBCs and the bursting size r by a factor of θ with $0 \le \theta \le 100\%$ representing the drug efficacy. To incorporate the drug efficacy of Malarone, we modify the 3rd-5th equations in model I in the way shown below and keep the other equations the same.

$$\begin{aligned}
\frac{\partial m(t,\nu)}{\partial t} + \frac{\partial m(t,\nu)}{\partial \nu} &= k_0 X(t) - \alpha_m(t,\nu,M(t))m(t,\nu) \\
&\quad - \frac{(1-\theta)k_1}{1+k_2A(t)}Y(t)m(t,\nu), \\
&\quad 0 < \nu < \nu_F, \\
\frac{dX(t)}{dt} &= \frac{(1-\theta)k_1}{1+k_2A(t)}Y(t)M(t) - s(t)X(t) - \alpha_x X(t) - k_3 I(t)X(t), \\
\frac{dY(t)}{dt} &= \frac{(1-\theta)r}{1+k_4 I(t)}s(t)X(t) - \alpha_y Y(t) - k_5 I(t)Y(t) \\
&\quad - \frac{(1-\theta)k_1}{1+k_2A(t)}Y(t)M(t),
\end{aligned} \tag{2.16}$$

Our simulation results in Fig. 12 show that administration of the drug Malarone has better treatment effects than Coartem and SP. RBC levels increase faster than the other two drugs while merozoites and infected RBCs decrease faster. If the drug efficacy reaches 80% or higher, the infection will be treated.

3. A prospect model for investigating severe malaria infections

3.1. The mathematical model

Malaria may rapidly become a severe case without prompt and appropriate treatment [35]. The major complications of severe malaria include cerebral malaria, pulmonary edema, acute renal failure, severe anemia, and/or bleeding. Acidosis and hypoglycemia are the most common metabolic complications [38]. Any of these complications can develop rapidly and progress to death within hours or days [38]. Immune clearance and the availability of infected RBCs in which the parasites develop and reproduce are two major factors that shape the peaks and troughs of malaria parasitemia and thus in turn affect disease severity and transmission [24]. Authors in [29] hypothesized that merozoites enter already infected RBCs to multiply faster due to the limited availability of uninfected RBCs to merozoites when total clogging of venules occurs in severe malaria. Their hypothesis was presented from a mathematical point of view to gain some understanding of severe malaria. We utilize this hypothesis in model I (2.10) to investigate how such a hypothesis would affect the host's erythropoiesis and the disease dynamics. A second model (**model II**) is propsed below to incorporate the double infection assumption.

$$
\begin{aligned}
\frac{dE(t)}{dt} &= f(t, M(t)) - \alpha_E(t, P(t))E(t),\\
\frac{\partial p(t,\mu)}{\partial t} + g(E(t))\frac{\partial p(t,\mu)}{\partial \mu} &= \sigma(t,\mu,E(t))p(t,\mu) - H(X_1(t))p(t,\mu),\\
&\quad 0 < \mu < \mu_F,\\
\frac{\partial m(t,\nu)}{\partial t} + \frac{\partial m(t,\nu)}{\partial \nu} &= k_0 X_1(t) - \alpha_m(t,\nu,M(t))m(t,\nu)\\
&\quad - \frac{k_1}{1+k_2A(t)}Y(t)m(t,\nu),\\
&\quad 0 < \nu < \nu_F,\\
\frac{dX_1(t)}{dt} &= \frac{k_1}{1+k_2A(t)}Y(t)M(t) - s_1(t)X_1(t) - \alpha_{x1}X_1(t)\\
&\quad - k_3 I(t)X_1(t) - \beta X_1(t)Y(t),\\
\frac{dX_2(t)}{dt} &= \beta X_1(t)Y(t) - s_2(t)X_2(t) - \alpha_{x2}X_2(t) - k_3 I(t)X_2(t),\\
\frac{dY(t)}{dt} &= \frac{r_1}{1+k_4 I(t)}s_1(t)X_1(t) + \frac{r_2}{1+k_4 I(t)}s_2(t)X_2(t)\\
&\quad - \alpha_y Y(t)\\
&\quad - k_5 I(t)Y(t) - \frac{k_1}{1+k_2A(t)}Y(t)M(t)\\
&\quad - \beta\Big(X_1(t)+X_2(t)\Big)Y(t),\\
\frac{dI(t)}{dt} &= \lambda_I(t) + \left(\frac{\lambda_x X_1(t)}{k_6+X_1(t)} + \frac{\lambda_y Y(t)}{k_7+Y(t)}\right)I(t) - \alpha_I I(t),\\
\frac{dA(t)}{dt} &= \eta I(t)\frac{Y(t)}{k_8+Y(t)} - \alpha_A A(t)Y(t),
\end{aligned}
\tag{3.1}
$$

with the same boundary conditions as in model I. Here, X_1 and X_2 are the population of newly infected RBCs and double infected RBCs, respectively. For newly infected RBCs we model the burst rate by s_1, the natural mortality rate by α_{x1}, and the average number of newly released merozoites upon rupture by r_1. Already infected RBCs could be infected for a second time by merozoites at a rate modeled by $\beta X_1 Y$. The double infected RBCs die off at a rate α_{x2}, rupture at a rate s_2, and release r_2 new merozoites per bursting.

3.2. A finite difference algorithm

Similar numerical treatments applied to solve model II (3.1) yield

$$
\begin{aligned}
\frac{E^{k+1}-E^k}{\Delta t} &= f^k - \alpha_E^k E^{k+1},\\
\frac{p_i^{k+1}-p_i^k}{\Delta t} + g^{k+1}\frac{p_i^k - p_{i-1}^k}{\Delta \mu} &= \sigma_i^{k+1}p_i^k - H(X_1^k)p_i^{k+1}, \quad i = 1,\dots,n_1,\\
\frac{m_j^{k+1}-m_j^k}{\Delta t} + \frac{m_j^k - m_{j-1}^k}{\Delta \nu} &= k_0 X_1^k - (\alpha_m)_j^k m_j^{k+1} - \frac{k_1}{1+k_2A^k}Y^k m_j^{k+1},\\
&\quad j = 1,\dots,n_2,\\
\frac{X_1^{k+1}-X_1^k}{\Delta t} &= \frac{k_1}{1+k_2A^k}Y^k M^{k+1} - s_1^{k+1}X_1^{k+1}\\
&\quad - \alpha_{x_1}X_1^{k+1} - k_3 I^k X_1^{k+1}\\
&\quad - \beta X_1^{k+1}Y^k,\\
\frac{X_2^{k+1}-X_2^k}{\Delta t} &= \beta X_1^{k+1}Y^k - s_2^{k+1}X_2^{k+1} - \alpha_{x_2}X_2^{k+1}\\
&\quad - k_3 I^k X_2^{k+1},\\
\frac{Y^{k+1}-Y^k}{\Delta t} &= \frac{r_1}{1+k_4 I^k}s_1^{k+1}X_1^{k+1} + \frac{r_2}{1+k_4 I^k}s_2^{k+1}X_2^{k+1}\\
&\quad - \alpha_y Y^{k+1}\\
&\quad - k_5 I^k Y^{k+1} - \frac{k_1}{1+k_2A^k}Y^{k+1}M^{k+1}\\
&\quad - \beta(X_1^{k+1}+X_2^{k+1})Y^{k+1},\\
\frac{I^{k+1}-I^k}{\Delta t} &= {\lambda_I}^{k+1} + \left(\frac{\lambda_x X_1^{k+1}}{k_6+X_1^{k+1}} + \frac{\lambda_y Y^{k+1}}{k_7+Y^{k+1}}\right)I^k\\
&\quad - \alpha_I I^{k+1},\\
\frac{A^{k+1}-A^k}{\Delta t} &= \eta I^{k+1}\frac{Y^{k+1}}{k_8+Y^{k+1}} - \alpha_A A^{k+1}Y^{k+1},\\
g^{k+1}p_0^{k+1} &= \phi^{k+1}E^{k+1},\\
m_0^{k+1} &= g^{k+1}p_{n_1}^{k+1}.
\end{aligned}
\tag{3.2}
$$

3.3. Simulation results

Simulations in [29] apply delayed rejection adaptive Markov chain Monte Carlo methods to determine parameter distribution in within-host severe *P. falciparum* malaria. In order to demonstrate the dynamics of severe malaria described by our model II (3.1) quantitatively, we adopt the sample means of their estimates regarding the following second infection parameters: $\alpha_{x_1} = 0.0241$, $\alpha_{x_2} = 0.1014$, $k_s = 2.5119 \times 10^{-10}$, $\beta = 2.0108 \times 10^{-10}$, $s_1 = 0.5$, $s_2 = 0.5$, $r_1 = 31.7924$, $r_2 = 27.6375$. The values of other parameters are the same as those shown in Table 3.

Simulation results are demonstrated in Fig. 13. It is observed that, if the merozoites enter already infected RBCs, they produce more merozoites shortly after the infection. Thus there is an increased chance of more RBC infection at the beginning of the infection. The double infection hypothesis dramatically affects the host's RBC production. The uninfected RBC population experiences a sharp decline shortly after the infection, which is a signal for the host's body to release more erythropoietin. This hormone then stimulates proliferation and differentiation of precursors. However, this increase in erythropoiesis fails to increase the abundance in uninfected RBC population since more merozoites are released. The uninfected RBC population remains at a low level after the infection. The results indicate that in case of double infection, the host may develop anemia.

4. Conclusions and discussion

In this work we developed two mathematical models to gain

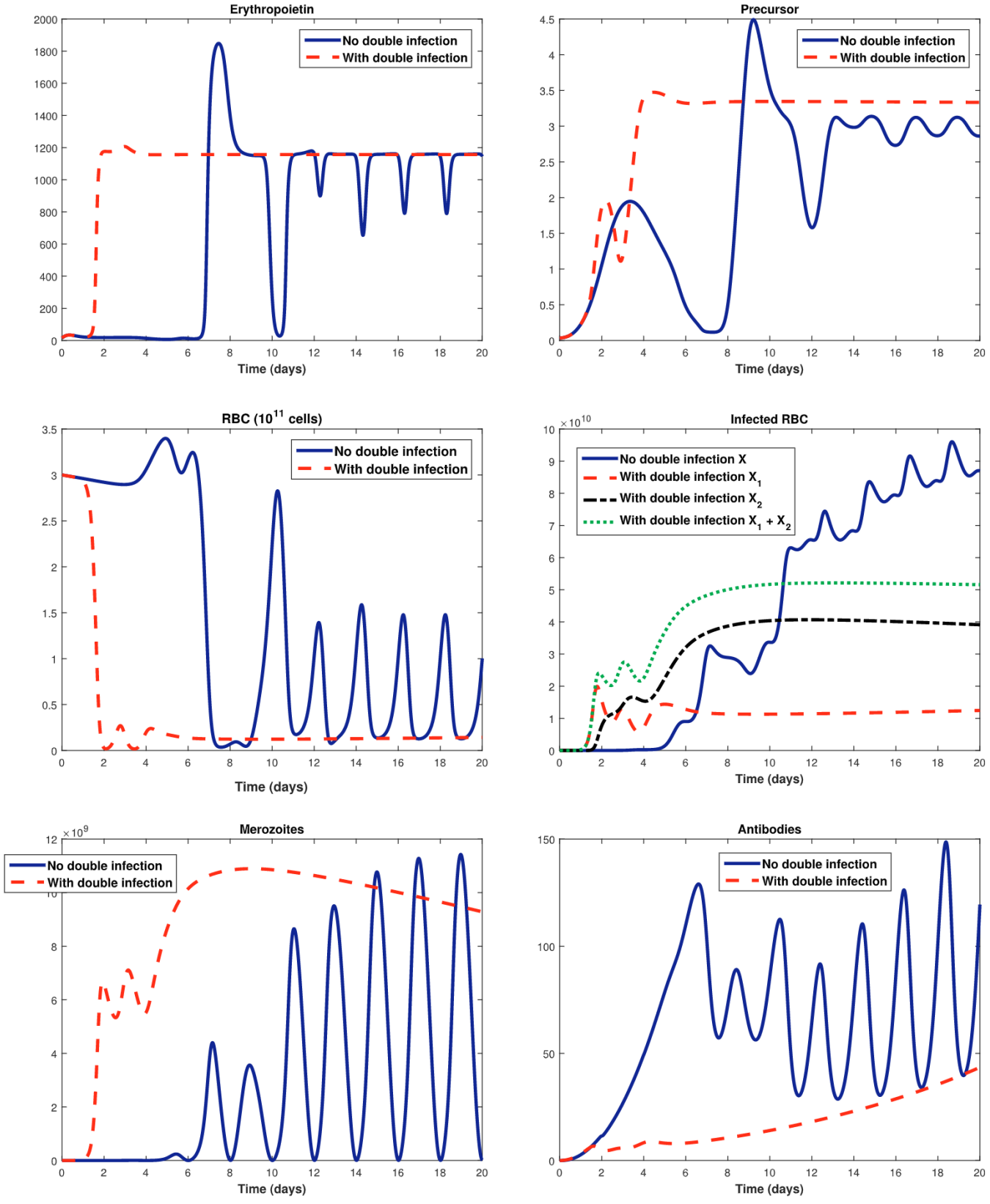

Fig. 13. Simulation of the dynamics of erythropoietin, precursor, RBCs, infected RBCs, merozoites, and antibodies in severe malaria with the assumption of double infection.

understanding of the complex system of within-host malaria infection. The first model (model I) describes the host's immune responses to *Plasmodium falciparum* infection as well as the process of erythropoiesis under the stress of malaria infection. The numerical simulation results demonstrate that natural host immune response is not able to control the malaria infection. Increasing the immunosensitivity/immunogenicity of infected RBC and merozoites does not effectively reduce the infection level nor does it keep the RBC at a healthy level. The

infected RBC and merozoite population experience only a slight decrease when increasing the efficiency of antibodies in blocking the parasite infection of healthy RBCs. Parameter sensitivity analysis shows that reducing the number of free merozoites released per infected RBC seems to be the most effective way of maintaining a healthy population of RBCs and controlling the disease. The disease dynamics is also very sensitive to parasite mortality rate and parasite infection rate. These simulation results are consistent with prior studies in literature [1,2,29].

We proposed a second mathematical model (model II) based on the assumptions that in severe infection some free merozoites in the blood stream enter already infected RBCs due to the limited availability of healthy RBCs [29]. Using the mean values of parameters estimated by authors in [29] we performed numerical simulations to investigate how such a hypothesis would affect the host's erythropoiesis and the disease dynamics during severe malaria infections. The results (as in Fig. 13) reveal that shortly after the infection, the RBCs decline sharply and remain low afterwards. More merozoites are produced compared to the case with no double infection, resulting in more RBCs being infected, which may result in anemia in the host. To our best knowledge, this is the first study of complex interactions between the processes of erythropoiesis, the malaria parasites, and the immune responses during severe malaria infection using mathematical models.

We also studied the effectiveness of various drugs, such as SP (Sulfadoxine/Pyrimethamine), Coartem (Artemether/lumefantrine), and Malarone (Atovaquone–Proguanil), for treating malaria utilizing model I. The administration of SP or Coartem will reduce the number of newly released merozoites per bursting infected RBCs, while Malarone will reduce parasite infection rate as well as the bursting size. Our simulation results demonstrate that the administration of these three drugs will effectively put the infection under control when the drug efficacy reach a certain level ($> 95\%$ for SP and Coartem and $> 75\%$ for Malarone). Moreover, Malarone has more significant treatment effects than SP or Coartem. However, our models only provide the disease dynamics under the treatment of a single drug. Drug resistance which is common and causes treatment failure is not considered in the models. Due to the spread of resistance, WHO recommends that a combination of drugs is used in treating malaria. For example, Malarone is recommended to be used only in combination with another anti-malarial compound since the resistance will occur very quickly when used in mono-therapy. Our models provide basic patterns in malaria infection and under drug treatment. These models help to gain insights to complex interactions of the within-host malaria infection, while more sophisticated models are desired for studying treatment by a combination of drugs and for including drug resistance in the treatment.

Acknowledgments

We thank anonymous referees for their helpful suggestions and comments. We also thank Cameron Compell for proof reading this work.

Supplementary material

Supplementary material associated with this article can be found, in the online version, at 10.1016/j.mbs.2019.02.005.

References

[1] A.S. Ackleh, K. Deng, K. Ito, J.J. Thibodeaux, A structured erythropoiesis model with nonlinear cell maturation velocity and hormone decay rate, Math. Biosci. 204 (2006) 21–48.
[2] A.S. Ackleh, B. Ma, J.J. Thibodeaux, A second-order high resolution finite difference scheme for a structured erythropoiesis model subject to malaria infection, Math. Biosci. 245 (2013) 2–11.
[3] R.M. Anderson, R.M. May, S. Gupta, Non-linear phenomena in host-parasite interactions, Parasitology 99 (1989) 59–79.
[4] K. Artavanis-Tsakonas, J.E. Tongren, E.M. Riley, The war between the malaria parasite and the immune system: immunity, immunoregulation and immunopathology, Clin. Exp. Immunol. 133 (2003) 145–152.
[5] J. Bélair, J.M. Mahaffy, Variable maturation velocity and parameter sensitivity in a model for hematopoiesis, IMA Math. Med. Biol. 18 (2001) 193–211.
[6] C. Casals-Pascual, O. Kai, J.O.P. Cheung, S. Williams, B. Lowe, M. Nyanoti, T.N. Williams, K. Maitland, M. Molyneux, C.R.J.C. Newton, N. Peshu, S.M. Watt, D.J. Roberts, Suppression of erythropoiesis in malarial anemia is associated with hemozoin in vitro and in vivo, Blood 108 (2006) 2569–2577.
[7] C. Chiyaka, W. Garira, S. Dube, Modelling immune response and drug therapy in human malaria infection, Comput. Math. Methods Med. 9 (2008) 143–163.
[8] H. Cordel, J. Cailhol, S. Matheron, M. Bloch, N. Godineau, P.H. Consigny, H. Gros, P. Campa, P. Bourée, O. Fain, P. Ralaimazava, O. Bouchaud, Atovaquone–Proguanil in the treatment of imported uncomplicated plasmodium falciparum malaria: a prospective observational study of 553 cases, Malar. J. 12 (2013), https://doi.org/10.1186/1475-2875-12-399.
[9] P. De Leenheer, S.S. Pilyugin, Immune response to a malaria infection: properties of a mathematical model, J. Biol. Dyn. 2 (2008) 102.
[10] D.L. Doolan, C.D. no, J.K. Baird, Acquired immunity to malaria, Clin. Microbiol. Rev. 22 (2009) 13–36.
[11] C.I. Fanello, C. Karema, W. van Doren, C.V. Overmeir, D. Ngamije D, U. D'Alessandro U, A randomised trial to assess the safety and efficacy of artemether-lumefantrine (coartem) for the treatment of uncomplicated plasmodium falciparum malaria in rwanda, Trans. R. Soc. Trop. Med. Hyg. 101 (2007) 344–350.
[12] J.F. Faucher, A. Aubouy, A. Adeothy, J. Doritchamou, G. Cottrell, B. Gourmel, et al., Comparison of sulfadoxine/pyrimethamine, unsupervised artemether-lumefantrine, and unsupervised artesunate-amodiaquine fixed-dose formulation for uncomplicated plasmodium falciparum malaria in benin: a randomized effectiveness noninferiority trial, J.Infect.Dis. 200 (2009) 57–65.
[13] J.L. Gallup, J.D. Sachs, The economic burden of malaria, Am. J. Trop. Med. Hyg. 64 (2001) 85–96.
[14] M.B. Gravenor, A.L. Lloyd, P.G. Kremsner, M.A. Missinou, M. English, K. Marsh, D. Kwiatkowski, A model for estimating total parasite load in falciparum malaria patients, J. Theor. Biol. 217 (2002) 137.
[15] B. Hellriegel, Modelling the immune response to malaria with ecological concepts: short-term behaviour against long-term equilibrium, Proc. R. Soc. London 250 (1992) 249–256.
[16] C. Hetze, R.M. Anderson, The within-host cellular dynamics of bloodstage malaria: theoretical and experimental studies, Parasitology 113 (1996) 25–38.
[17] S.L. Hoffman, Malaria Vaccine Development, ASM Press, Washington, DC, 1996.
[18] M.B. Hoshen, R. Heinrich, W.D. Stein, H. Ginsburg, Mathematical modelling of the within-host dynamics of *Plasmodium falciparum*, Parasitology 121 (2000) 227–235.
[19] A. Iggidr, J.-C. Kamgang, G. Sallet, J.-J. Tewa, Global analysis of new malaria intrahost models with a competitive exclusion principle, SIAM J. Appl. Math. 67 (2006) 260.
[20] C.A.Jr. Janeway, P. Travers, M. Walport, M. Shlomchik, M. Schlomchik, Immunobiology: The Immune System in Health and Disease, 5th, Garland Science Press, New York, 2001.
[21] B. Kamangira, P. Nyamugure, G. Magombedze, A theoretical mathematical assessment of the effectiveness of coartemether in the treatment of plasmodium falciparum malaria infection, Math. Biosci. 256 (2014) 28–41.
[22] F.O. ter Kuile, A.M. van Eijk, S.J. Filler, Effect of sulfadoxine/pyrimethamine resistance on the efficacy of intermittent preventive therapy for malaria control during pregnancy: a systematic review, JAMA 297 (2007) 2603–2616.
[23] J.M. Mahaffy, S.W. Polk, R.K.W. Roeder, An age-structured model for erythropoiesis following a phlebotomy, Technical report, (1999). CRM-2598
[24] C.J.E. Metcalf, A.L. Graham, S. Huijben, V.C. Barclay, G.H. Long, B.T. Grenfell, A.F. Read, O.N. Bjørnstad, Partitioning regulatory mechanisms of within-host malaria dynamics using the effective propagation number, Science 333 (2011) 984–988.
[25] L. Molineaux, H.H. Diebner, M. Eichner, W.E. Collins, G.M. Jeffery, K. Dietz, *Plasmodium falciparum* parasitaemia described by a new mathematical model, Parasitology 122 (2001) 379–391.
[26] L. Molineaux, K. Dietz, Review of intra-host models of malaria, Parassitologia 41 (1999) 221–231.
[27] M. Mulenga, J.-P.V. geertruyden, L. Mwananyanda, V. Chalwe, F. Moerman, R. Chilengi, C.V. Overmeir, J.-C. Dujardin, U. D'Alessandro, Safety and efficacy of lumefantrine-artemether (coartem®) for the treatment of uncomplicated *Plasmodium falciparum* malaria in zambian adults, Malar. J. 5 (2006) 73.
[28] S.C. Murphy, J.G. Breman, Gaps in the childhood malaria burden in africa: cerebral malaria, neurological sequelae, anemia, respiratory distress, hypoglycemia, and complications of pregnancy, Am. J. Trop. Med. Hyg. 64 (2001) 57–67.
[29] B. Nannyonga, G.G. Mwanga, H. Haario, I.S. Mbalawata, M. Heilio, Determining parameter distribution in within-host severe *p. falciparum* malaria, BioSystems 126 (2014) 76–84.
[30] Understanding Malaria, (2007). No. 07–7139
[31] M. Recker, C.O. Buckee, A. Serazin, S. Kyes, R. Pinches, Z. Christodoulou, A.L. Springer, S. Gupta, C.I. Newbold, Antigenic variation in *Plasmodium falciparum*malaria involves a highly structured switching pattern, PLoS Pathog. 7 (2011) e1001306, https://doi.org/10.1371/journal.ppat.1001306.
[32] I.W. Sherman, Malaria: Parasite Biology, Pathogenesis and Protection, ASM Press, Washington, DC, 1998.
[33] C.E. Shulman, E.K. Dorman, F. Cutts, K. Kawuondo, J.N. Bulmer, N. Peshu, et al., Intermittent sulphadoxine-pyrimethamine to prevent severe anaemia secondary to malaria in pregnancy: a randomised placebo-controlled trial, Lancet 9153 (1999) 632–636.

[34] J.J. Thibodeaux, Modeling erythropoiesis subject to malaria infection, Math. Biosci. 225 (2010) 59–67.
[35] A. Trampuz, M. Jereb, I. Muzlovic, R.M. Prabhu, Clinical review: severe malaria, Crit.Care 7 (2003) 315–323.
[36] J. Tumwiine, S. Luckhaus, J.Y.T. Mugisha, L.S. Luboobi, An age-structured mathematical model for the within host dynamics of malaria and the immune system, J. Math. Modell. Algorithms 7 (2008) 79–97.
[37] J. Tumwiine, J.Y.T. Mugisha, L.S. Luboobi, On global stability of the intra-host dynamics of malaria and the immune system, J. Math. Anal. Appl. 341 (2008) 855–869.
[38] WHO, Severe malaria, Trop. Med. Int. Health 19 (Suppl. 1) (2014) 7–131.
[39] WHO, World health organization WHO expert committee on malaria, Twentieth report, *World Health Organization*, 2000. Technical Report Series
[40] WHO, World Malaria Report, (2013). www.who.int/malaria/publications/world_malaria_report_2013/en.
[41] S.N. Wickramasinghe, S.H. Abdalla, Blood and bone marrow changes in malaria, Best Pract. Res. Clin. Haematol. 13 (2000) 277–299.